

Ligands for the Tyrosine Kinase p56^{lck} SH2 Domain: Discovery of Potent Dipeptide Derivatives with Monocharged, Nonhydrolyzable Phosphate Replacements

Pierre L. Beaulieu,* Dale R. Cameron, Jean-Marie Ferland, Jean Gauthier, Elise Ghro, James Gillard, Vida Gorys, Martin Poirier, Jean Rancourt, Dominik Wernic, and Montse Llinas-Brunet

Boehringer Ingelheim (Canada) Ltd., Bio-Mega Research Division, 2100 Cunard Street, Laval, Québec H7S 2G5, Canada

Raj Betageri, Mario Cardozo, Eugene R. Hickey, Richard Ingraham, Scott Jakes, Alisa Kabcenell, Tom Kirrane, Susan Lukas, Usha Patel, John Proudfoot, Rajiv Sharma, Liang Tong,[†] and Neil Moss

Boehringer Ingelheim Pharmaceuticals Inc., 175 Briar Ridge Road, Ridgefield, Connecticut 06877

Received December 3, 1998

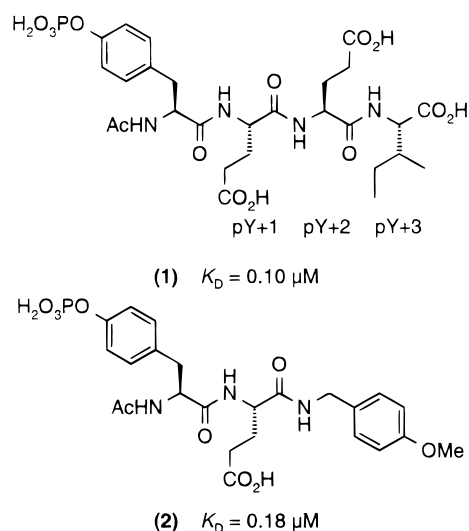
p56^{lck} is a member of the *src* family of tyrosine kinases. Through modular binding units called SH2 domains, p56^{lck} promotes phosphotyrosine-dependent protein–protein interactions and plays a critical role in signal transduction events that lead to T-cell activation. Starting from the phosphorylated dipeptide (**2**), a high-affinity ligand for the p56^{lck} SH2 domain, we have designed novel dipeptides that contain monocharged, nonhydrolyzable phosphate group replacements and bind to the protein with K_D 's in the low micromolar range. Replacement of the phosphate group in phosphotyrosine-containing sequences by a (*R/S*)-hydroxyacetic (compound **8**) or an oxamic acid (compound **10**) moiety leads to hydrolytically stable, monocharged ligands, with 83- and 233-fold decreases in potency, respectively. This loss in binding affinity can be partially compensated for by incorporating large lipophilic groups at the inhibitor N-terminus. These groups provide up to 13-fold increases in potency depending on the nature of the phosphate replacement. The discovery of potent (2–3 μ M), hydrolytically stable dipeptide derivatives, bearing only two charges at physiological pH, represents a significant step toward the discovery of compounds with cellular activity and the development of novel therapeutics for conditions associated with undesired T-cell proliferation.

Introduction

p56^{lck}, a member of the *src* family of tyrosine kinases,¹ is predominantly expressed in T lymphocytes where it plays a critical role in T-cell-mediated immune responses.² Upon recognition of an antigen by the T-cell antigen receptor (TCR), an intracellular cascade of signal transduction events is initiated, which ultimately leads to T-cell activation. p56^{lck} is implicated in the early phase of TCR activation, through the tyrosine phosphorylation of intracellular proteins. This phosphorylation can serve as an allosteric regulatory event or can initiate protein–protein interactions through SH2 domains.³

SH2 domains are noncatalytic modules of about 100 amino acids, conserved among a large number of signal transduction proteins.⁴ Controlled intracellular signaling events are initiated by the binding of SH2 domains to specific phosphotyrosine-containing protein sequences. The involvement of an SH2 domain in the steps leading to T-cell activation makes this protein an attractive target for pharmaceutical intervention. The specificity of interaction for the *src* family of SH2 domains is highly dependent on the three amino acid residues immediately adjacent to the C-terminal side of the phosphorylated tyrosine.⁵ The SH2 domain of p56^{lck} displays high affinity for peptide sequences containing pYEEI (pY = phosphotyrosine),^{5,6} and the crystal structure of Ac-

Chart 1



pYEEI-OH (**1**) (Chart 1) complexed with the SH2 domain of p56^{lck} has been published.^{7–9} The structure reveals strong interactions between basic residues on the protein and the phosphorylated tyrosine through an intricate hydrogen-bond network. The Ile side chain fits in a well-defined hydrophobic pocket on the protein.

The affinity of tetrapeptide **1**, for the SH2 domain of p56^{lck} ($K_D = 100 \text{ nM}$),¹⁰ made it an attractive lead structure for the rational design of agents to compete

[†] Present address: Department of Biological Sciences, Columbia University, 1212 Amsterdam Ave, New York, NY 10027.

with the SH2 domain's natural ligands. Such agents could be effective for the control of autoimmune diseases, such as multiple sclerosis and rheumatoid arthritis, and organ transplant rejection phenomena. To produce a therapeutic effect, an SH2 domain antagonist has to be able to reach efficacious concentrations inside cells. Unfortunately, tetrapeptide **1** does not elicit response in cell-based assays of T-cell activation. Compound **1** has several undesirable features that may account for this: (a) the phosphate group, an essential element for binding to the SH2 domain, is metabolically unstable to phosphatases present in cells¹¹ and (b) the five negative charges at physiological pH and the high peptidic character of compound **1** (i.e., four amide bonds) may limit its ability to reach efficacious concentrations inside the cell. Attempts to address these issues have appeared in the literature for the related *src* SH2 domain.¹² Nonhydrolyzable phosphate mimics have been reported,¹³ peptidomimetics of reduced size and charge have been designed,¹⁴ and prodrug approaches to achieving efficacious concentrations inside cells have been explored.^{12,13d} However, achieving efficacy in a cell-based assay has not been generally reported.¹⁵

Previously, we described the development of phosphorylated dipeptide **2** (Chart 1) in which the pY+2 to pY+3 portion of **1** (Glu-Ile-OH) was replaced by a (4-methoxybenzyl)amide group. Compound **2**, which has two less carboxylic acid groups and one less amide linkage than the lead structure, showed good affinity ($K_D = 180$ nM) for the *Ick* SH2 domain.¹⁶ Parallel with these studies, we were also searching for metabolically stable phosphate group replacements of minimal charge that would provide high binding affinity within the phosphate binding pocket of p56^{*lck*} SH2.

Results and Discussion

Phosphate Group Replacements. The X-ray crystal structure of **1** complexed to the p56^{*lck*} SH2 domain reveals a pocket exquisitely adapted for the binding of the phosphotyrosyl moiety (Figure 1).⁹ The phosphate group of **1** is involved in an intricate network of hydrogen bonding and electrostatic interactions with the protein. As depicted in Figure 1, two of the phosphate oxygen atoms participate in tetrahedral hydrogen-bonding arrangements with the protein (main chain amide N-H of Glu157, guanidinium groups of Arg134 and Arg154, and side chain OH of Ser164). The third oxygen atom hydrogen bonds with the side chain OH of Ser158. The aromatic ring of the phosphotyrosine residue faces the side-chain guanidinium group of Arg134 and is involved in a stabilizing amino–aromatic interaction.¹⁷

The design of high-affinity, stable, and minimally charged phosphate group replacements has met with limited success, and this presents a major obstacle to the development of novel therapeutics based on phosphopeptide mimetics. To date, only closely related difluoromethylphosphonate derivatives retain good binding affinity while providing metabolic stability.^{12b,13d} Unfortunately, the incorporation of this entity into peptidomimetic-based ligands has not generally resulted in compounds with cellular activity, presumably because it retains two negative charges at physiological pH that impede cell permeation (as is the case with phosphotyrosine-based compounds).

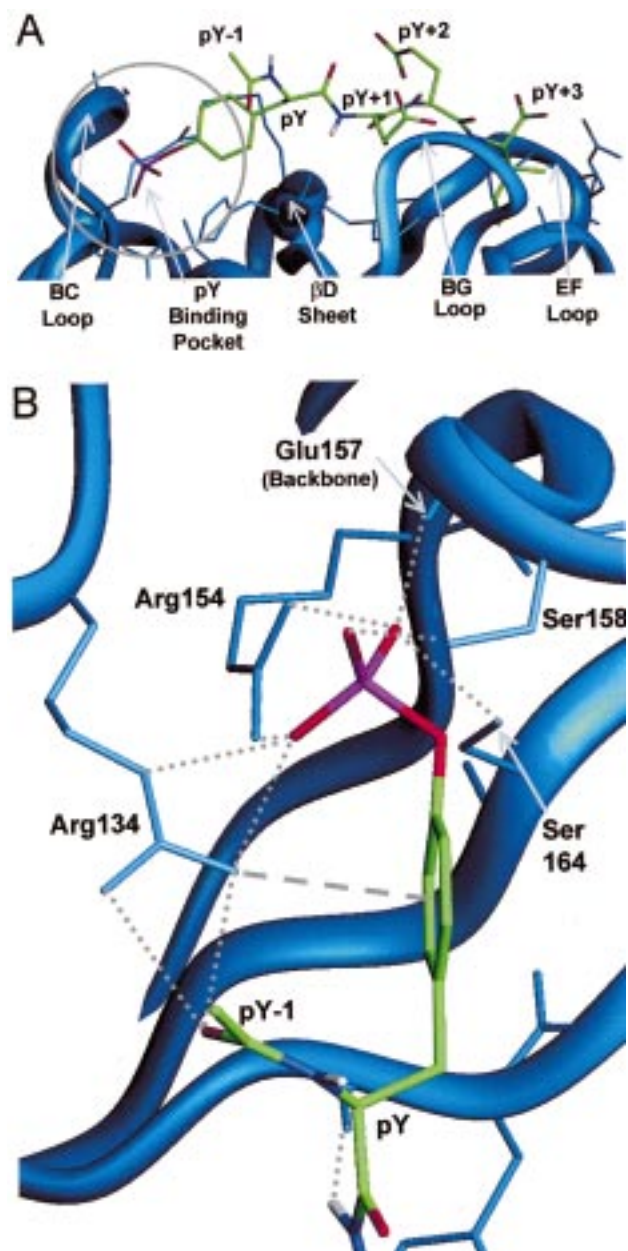
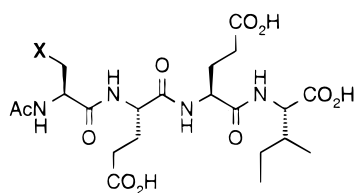


Figure 1. (A) Binding pocket of the p56^{*lck*} SH2 domain is highlighted. The pY binding pocket is contained between loop BC and sheet β D. The pY+3 binding pocket is located in a hydrophobic cleft between loops BG and EF. The protein backbone is highlighted as a ribbon, and side chains are shown in blue (without hydrogens). The ligand (**1**) is colored by atom type as follows: carbon, green; oxygen, red; nitrogen, dark blue; phosphorus, violet. (B) Hydrogen bonding in the pY pocket (hydrogen bonds are shown as dotted lines between heavy atoms). The π -cation interaction between pY and Arg134 is shown with a dashed line.

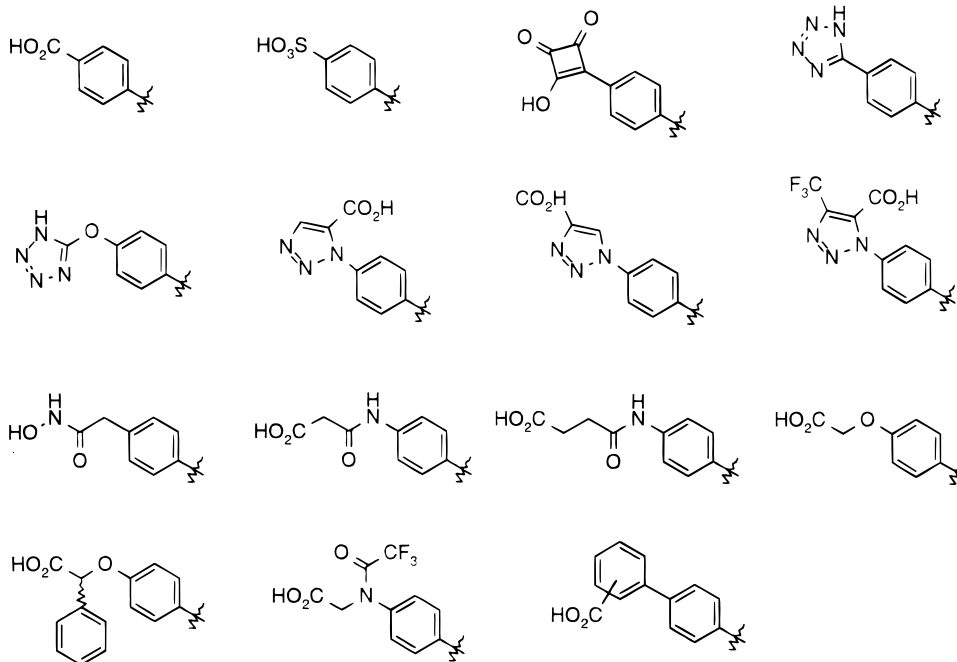
In our efforts to identify suitable phosphate replacements, a large number of substituted phenylalanine derivatives were incorporated into Ac-pYEEI (**1**) in place of the phosphotyrosine residue. Several examples are shown in Chart 2. They include functionality that would be expected to carry either one or no charges at physiological pH. Despite the potential for some of these entities to set up strong electrostatic or hydrogen-bonding interactions within the hydrophilic binding pocket of the SH2 protein, none of the compounds showed binding when tested at 100 μ M concentration.

Chart 2



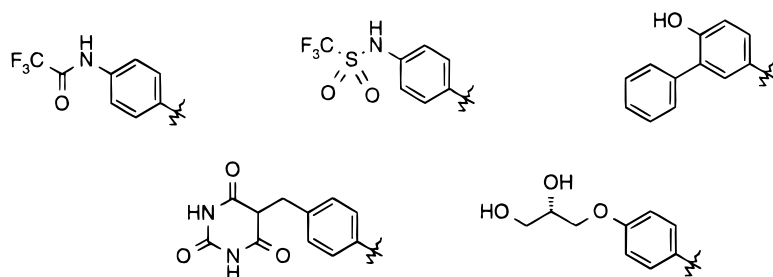
Phosphate replacements with one ionizable group

X =



Phosphate replacements with no ionizable group

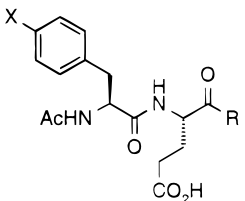
X =

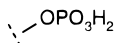
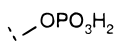
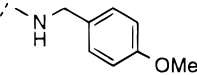
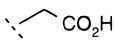

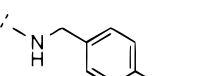


It thus became apparent that finding even a mono-charged phosphate replacement that maintains reasonable potency would be a difficult task. It seemed inevitable that if we wanted, at most, a mono-charged phosphate replacement, we would have to work with a significantly less potent ligand and thus would need to compensate by optimization of binding interactions with other parts of the molecule.

The acetic acid moiety ($\text{CH}_2\text{CO}_2\text{H}$) has been evaluated as a phosphate group replacement and, within the context of a *src* SH2 domain interaction, results in an approximately 1000-fold decrease in binding affinity, relative to the corresponding phosphate or difluoromethylphosphonate analogues.^{8d,12c} In the case of p56^{lck} SH2, this replacement (compound **3**, Table 1) resulted in a similar decrease in binding affinity. We were

initially concerned that the large difference in binding affinity between **1** and **3** might reflect significantly different modes of interaction with the protein. However, the X-ray crystal structure of a complex between **3** and the p56^{lck} SH2 domain reveals that **3** binds in a similar extended fashion to phosphopeptide **1** (Figure 2).¹⁸ The bound conformations of the pY+3 Ile residues were almost identical in the two analogues, the hydrogen-bonding interaction at pY+1 was retained, and the acetic acid side chain of **3** participates in many of the interactions characteristic of the phosphate group. The carboxylate oxygen atoms of **3** are almost superimposable with two of the phosphate oxygen atoms, maintaining interactions with the SH2 protein (Figure 2). Small conformational differences were observed between the phenyl rings of the two ligands and in the protein

Table 1


entry	X	R	K_D (μM)
1		Glu-Ile-OH	0.1
2			0.2
3		Glu-Ile-OH	42
4			50

backbone itself. The differences in affinity between phosphate **1** and phenylacetic derivative **3** are most likely due to a combination of factors. The less charged acetic acid group would be expected to have a weaker electrostatic interaction with the SH2 domain, and hydrogen bonding to Ser158 is lost. Also, the bound conformation of **3** may not be the most energetically favored. The observed 16° torsional angle across the carboxylate group and the plane of the phenyl ring results in a steric repulsion between the two groups.^{18,19} Finally, the difference in geometry imparted by the change in hybridization between the sp^3 phosphate group and the sp^2 carboxyl group may result in a less optimal hydrogen-bonding network.

Replacement of the phosphate group of **2** with an acetic acid moiety gave compound **4** with a K_D of $50 \mu\text{M}$ (Table 1). The comparable potencies observed in both the "long" and "short" series (compare entries **1** and **3** vs **2** and **4**) provided additional evidence that both phosphate and acetic acid derivatives were binding in a similar fashion. Compound **4**, a dipeptide containing only two ionizable groups at physiological pH and having a $K_D = 50 \mu\text{M}$ for the p56^{lck} SH2 domain, was used as a reference point for the evaluation of new ligands containing nonhydrolyzable, monocharged mimics of phosphotyrosine.

Extension of the acetic acid side chain of **4** by one methylene unit gave derivative **5** (Table 2) which was 4 times less potent ($K_D = 184 \mu\text{M}$). This result, in addition to the fact that the corresponding formic acid derivative (carboxyl directly attached to benzene ring, Chart 2) was >500 -fold less potent, indicates that a one-methylene spacer is better than two or none for maximal interaction within the phosphotyrosine binding pocket.

Table 2 also highlights several analogues of **4** substituted α to the carboxyl group. The difluoroacetic acid analogue **6** ($K_D = 166 \mu\text{M}$) is 3-fold less potent than **4**. This decrease could be a result of the weaker H-bonding ability of a difluoroacetate vs an acetate group. Introduction of a carbonyl α to the carboxylate group (derivative **7**) was predicted to better favor the binding

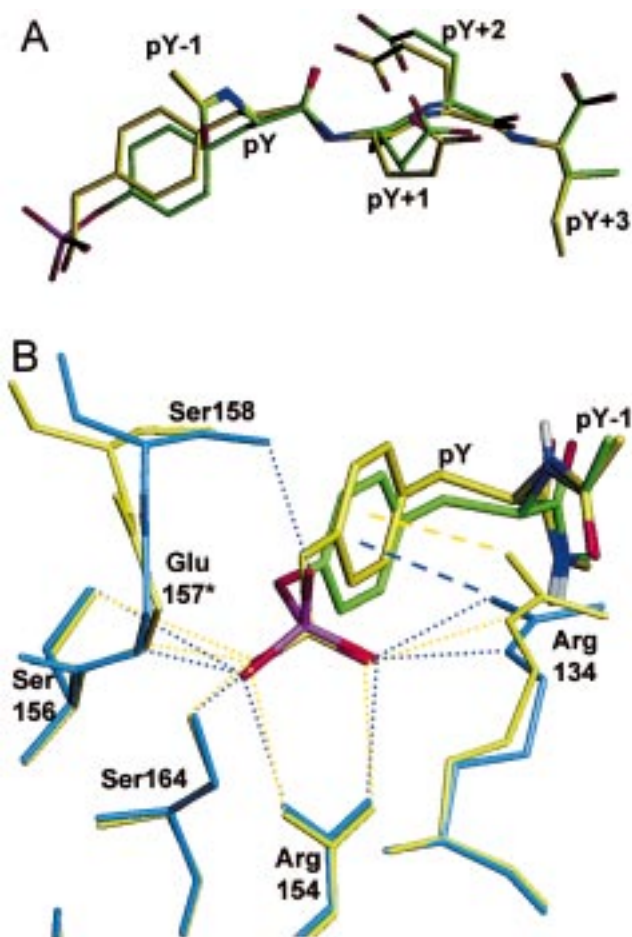


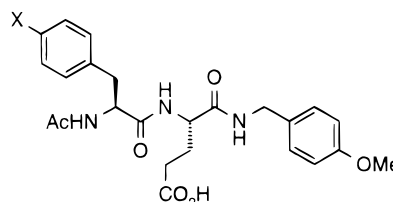
Figure 2. (A) Bound crystal structures for **1** and **3** complexed to the p56^{lck} SH2 domain show good overlap of the pY and pY+3 groups (**1** and **3** are colored as in Figure 1 except the carbons in **3** have been colored yellow). (B) Close-up view of the pY groups clearly shows the two oxygen atoms of the acetate group of **3** overlapping two of the oxygens of the phosphate group of **1**. One principal difference is the loss of the hydrogen bond with Ser158 in the case of **3** (the protein is colored blue for **1** and yellow for **3**). Hydrogen bonds with protein side chains are shown as small blue dotted lines for **1** and small yellow dashed lines for **3**. Possible π -cation effects are indicated with large dashed lines using the same color coding. Stars indicate no side chain shown.

conformation found for compound **4**.^{18,20} However, compound **7** was essentially equipotent to phenylacetic acid derivative **4** ($K_D = 65 \mu\text{M}$). It is conceivable that a decrease in pK_a of the carboxylic acid in **7** due to the electron-withdrawing keto group, changes in the orientation of the carboxylate group, or solvation/desolvation phenomena may compensate for any benefit gained by a favorable binding conformation.

An α -hydroxyl group (compound **8**, $K_D = 15 \mu\text{M}$, 1:1 mixture of epimers) on the other hand improves potency 3-fold relative to **4**. This increase in affinity could be the result of a hydrogen bond between the hydroxyl group and the side chain of Ser158 or an orienting (entropic) effect on the positioning of the carboxyl group. α -Hydroxyphosphonates are similarly more potent than phosphonates in the context of *src* SH2 domain ligands.^{8d}

Replacement of the side chain carboxyl group of **4** by a sulfonic acid moiety resulted in a 2-fold increase in potency (compound **9**, $K_D = 25 \mu\text{M}$), similar to what was seen previously in the context of other SH2 domains.^{8d}

Table 2



entry	X	K _D (μM)
2		0.2
4		50
5		184
6		166
7		65
8		15
9		25
10		42

Hoping to improve further the potency of this derivative, we attempted the preparation of the corresponding hydroxymethylsulfonic acid analogue (formally, the bisulfite adduct of a phenylalanine-4-carboxaldehyde residue). However, this entity proved unstable, and the desired analogue could not be isolated.

In our attempts to identify acidic substituents capable of extensive hydrogen-bonding patterns, we designed compound **10** containing an oxamic acid group as a novel phosphate replacement. This functional group conferred potency ($K_D = 42 \mu\text{M}$) equal to that of the acetic acid side chain of **4**, despite an increase in acidity ($\text{p}K_a \sim 2.2$ – 2.5 vs ~ 4.5 for **4**).²¹

Because of its novelty, ease of synthesis, and potential utility as a phosphate mimic, we undertook studies to further elucidate its mode of interaction with the phosphotyrosine binding pocket, and we also used it as a standard fragment to evaluate modifications at the N-terminus as described in detail below.

Model for Binding of Oxamic Derivatives to the p56^{lck} SH2 Domain. Despite our success in obtaining crystal structures of compounds **1** and **3** in complex with the SH2 domain, we have so far not been able to obtain suitable crystals of ligands containing the oxamic acid phosphate replacement. Nevertheless, because of its novelty as a phosphate replacement, we endeavored to model an oxamic acid-containing compound using the high-resolution protein structure previously obtained for **1**.⁹

N-Ac-Phe(4-NHCOCOOH)-NHMe was docked flexibly into the protein and then solvated by a sphere of water. The protein and docked ligand were then minimized in a series of steps. The resulting complex was then modified to generate **10**, followed again by solvation and minimization to generate a model of **10**, bound to the p56^{lck} SH2 domain. From this model, it could be seen that the oxamic acid group was situated deep in the pY binding pocket and made extensive hydrogen-bond contacts with the protein. Figure 3 outlines the hydrogen-bonding pattern of the N-acetyl-phosphotyrosine portion of **1** (X-ray structure) and the oxamic acid-phenylalanine portion of **10** (model structure) inside the phosphate binding pocket.

All three oxygens of the oxamic acid are involved in hydrogen bonds with the phosphate binding pocket. The amide carbonyl oxygen and one of the carboxyl oxygens are very close to the position of two phosphate oxygens that are involved in numerous hydrogen bonds to both Arg134 and Arg154 (Figure 4). This is in contrast to **3** where both carboxyl oxygens were involved in hydrogen bonding to Arg134 and Arg154 (Figure 2).

Although calculations show that phenyl-oxamic acid exists primarily in an all-planar conformation in the gas phase,²² when solvation effects are included, as in the PM3-SM3 method,²³ a nonplanar arrangement is preferred. In fact, the bound conformation observed in our final minimized model is very close to the predicted PM3-SM3 global minimum. The energy difference is approximately 1 kcal/mol and is mainly due to a small rotation of the carboxyl group to more properly fit the pocket.

The oxamic acid group extends further away from the phenyl ring than does either the phosphate or the carboxymethyl replacement, and this leads to two effects. First, one of the carboxyl oxygens of **10** is positioned deeper into the protein and consequently can make a new hydrogen-bond interaction with the backbone NH of Ser158. In addition, a modified interaction with the side chain of Ser158 is now possible with the NH of the oxamic acid group, switching the role of Ser158 side chain to a hydrogen-bond acceptor. Second, to accommodate the oxamic acid, the adjacent phenyl ring is positioned differently than that observed for either the phosphate or carboxymethyl compounds. Although the phenyl ring appears slightly displaced out of the pocket, Arg134 has also moved slightly and rotated to maintain the amine–aromatic interaction (Figure 4). This displacement does not appear to affect hydrogen bonds to pY and the pY+1 backbone. The more dramatic difference is in the placement of the pY-1 N-acetyl group. The carbonyl moiety of this group is involved in a hydrogen bond with Arg134 in the phosphate structure (Figure 3), but in the oxamate model, this has been replaced by a water-mediated hydrogen bond to Arg134. This different positioning for the N-terminus may explain some key differences we observe with N-terminal substitutions when comparing results from different phosphate mimics (see the following section).

Finally, the pY+1 Glu residue of **1**, **3**, and the model of **10** overlap very well (Figure 5). As was seen previously in the case of compound **2**,¹⁶ the 4-methoxybenzylamine phenyl ring of **10** essentially replaces the

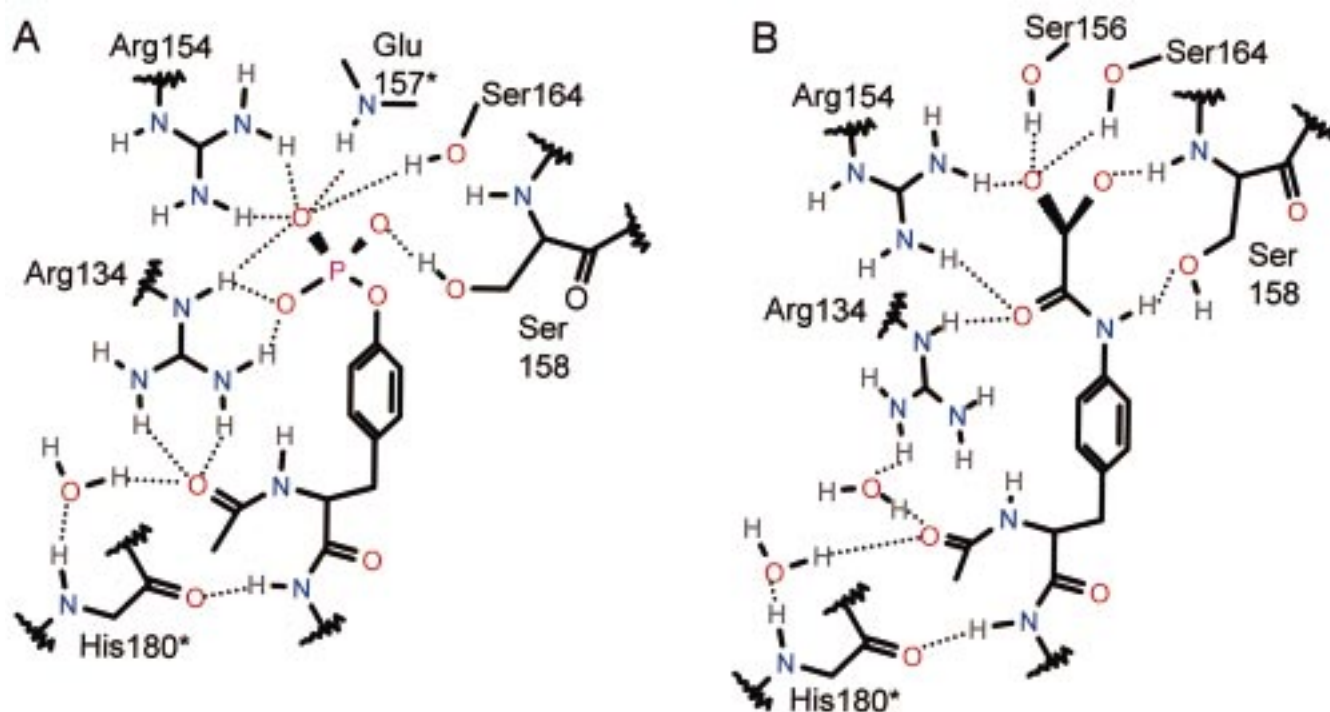


Figure 3. Hydrogen-bonding network for the pY groups of (A) **1** (X-ray structure) and (B) **10** (model structure) when bound to p56^{lck} SH2 domain. Although the oxamic acid group extends deeper inside the pY binding pocket, this group maintains a similar hydrogen-bonding network to **1**. Arg134 has moved significantly but still maintains hydrogen bonds in the pY pocket (see also Figure 4). Stars indicate no side chain shown.

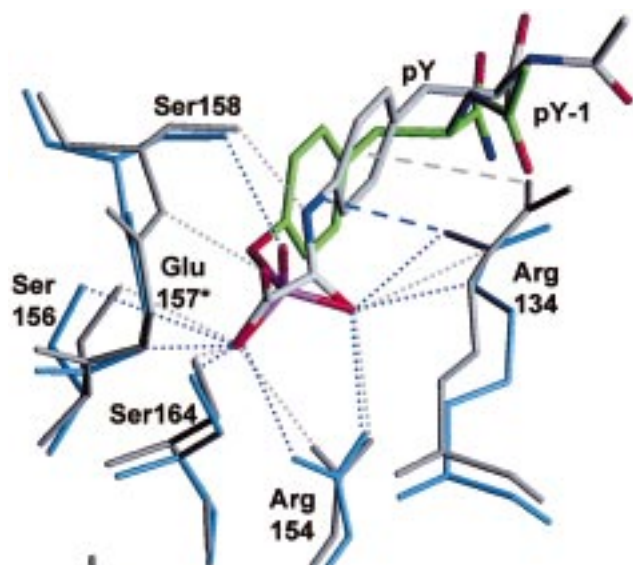


Figure 4. Superimposed pY groups of **1** (X-ray structure) and **10** (model structure) when bound to the p56^{lck} SH2 domain. Interactions with Arg154 and Ser158 are shown (note that in the case of **10**, the serine side chain is accepting a proton rather than donating). The phenyl ring of **10** has rotated causing a movement of the Arg134 side chain. **1** and its protein are colored as in Figure 1. The carbon atoms of **10** and its protein are colored gray. Stars indicate no side chain shown.

pY+2–pY+3 amide bond of **1** and **3**, allowing the *p*-methoxy group to occupy approximately the same area as the Ile side chain. Although there are some differences between the peptidic portions of the bound model for **10** and the structures of **1** and **3**, Figure 5 highlights clearly that **10** can effectively bind in a “two-pronged” fashion to mimic both the pY group and the pY+3 Ile.

Optimization of the Ligand N-Terminus. As we expected at the outset of this work, replacement of the phosphate group in our p56^{lck} SH2 domain antagonists by monocharged entities resulted in significant decreases in binding affinities (80–300-fold). The resulting dipeptide derivatives, however, had acquired metabolic stability and contained only two ionizable groups. We had indications in our early studies on phosphotyrosine-containing compounds (unpublished data) that additions to the N-terminus could improve potency. We reexamined these findings and used *N*-acetyloxamic acid derivative **10** ($K_D = 42 \mu\text{M}$) as a reference point due to its ease of synthesis and comparable potency to phenylacetic acid analogues **4** and **8** or sulfonic acid **9**. The highlights of an early optimization study are shown in Table 3. Consistent with our early work, while replacement of the *N*-acetyl group in **10** by a benzoyl moiety (compound **11**, Table 3) had little effect on potency, extending the phenyl ring from the N-terminal carbonyl by one or two methylenes improved potency 2–3-fold (compounds **12** and **13**). This encouraged the investigation of larger aromatic groups, and we discovered that incorporation of a naphthyl group could further increase potency another 4–5-fold (cf. compounds **14** and **15**, K_D 's $\sim 3 \mu\text{M}$). This prompted an extensive evaluation of further functionalized N-terminal groups to see if potency could be increased beyond $3 \mu\text{M}$ (results not shown). Examples included phenylacetamide, phenylpropionamide, and naphthylacetamide derivatives substituted with a variety of functional groups (amine, halogen, alkyl, nitro, hydroxyl) as well as quinoline, indole, and other heterocyclic derivatives. While some had comparable potency, none proved superior to the naphthylacetyl group of compounds **14** and **15**. A solid explanation why these N-terminal groups improve

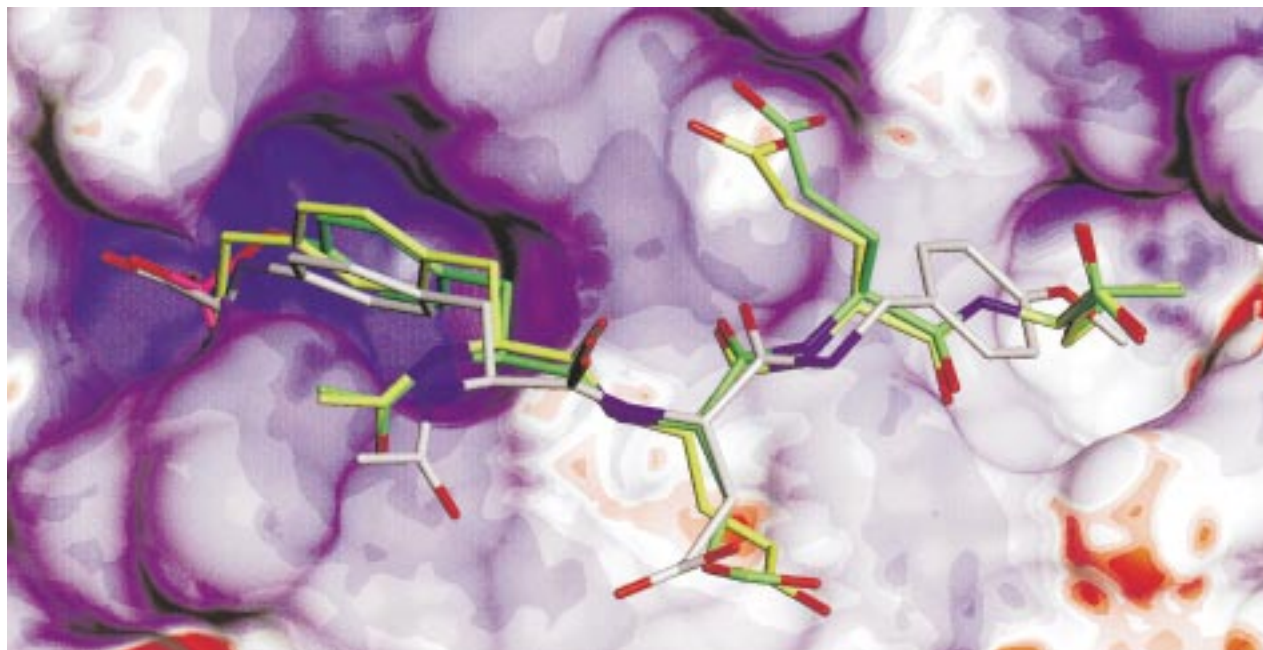


Figure 5. Superimposition of **1** and **3** (X-ray structures) and **10** (model structure), inside the solvent-accessible binding pocket of the p56^{lck} SH2 domain (generated from the complex with **1**).⁹ The “two-pronged” binding mode (pY and pY+3) of the three inhibitors is clearly visible. The backbones for the three ligands closely overlap, positioning the Ile side chain of **1** and **3** and the 4-methoxybenzyl group of **10** deep inside the pY+3 pocket. The surface is colored by charge distribution generated by performing a Poisson–Boltzmann calculation on the X-ray structure of the complex with **1** using Delphi (Molecular Simulations Inc.). The surface is colored with dark blue and red, corresponding to values of -5 and 15 kcal/mol, respectively.

Table 3

entry	R	K_b (μM)
10	Ac	42
11		32
12		17
13		13
14		3
15		3

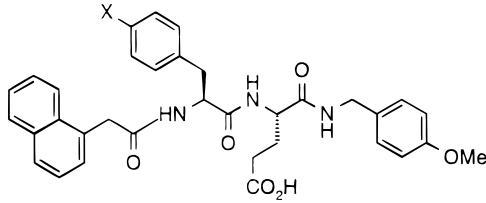
potency has proven somewhat elusive. An X-ray crystal structure of a complex of the p56^{lck} SH2 domain with phosphotrapeptide **1** in which the N-terminal acetyl group is replaced with a 1-naphthylacetyl group has

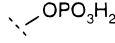
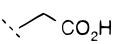
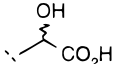
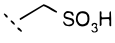
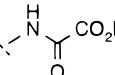
been solved.²⁴ Interestingly, both **1** and this latter compound interact with the protein in a similar fashion. However, the position of the naphthylacetyl group in the latter is not well-resolved, nor is it involved in any defined contact with the protein. Similar, yet more pronounced (100-fold), increases in potency are reported in the case of Grb2 SH2 domain binding sequences.²⁵ This result is rationalized based on molecular modeling which suggests a favorable planar π -stacking interaction between a 3-aminobenzoyloxycarbonyl N-terminus and an arginine residue and a strong intramolecular interaction between the 3-amino substituent and the phosphotyrosine residue.

Comparison of the data presented in Tables 2 and 4 reveals that the effect of the 1-naphthylacetyl group is more pronounced in the case of phosphate mimics than with phosphate. For instance, while the increase in potency is 4.5-fold in the case of phosphotyrosine (cf. **2** and **16**), a 7–11-fold increase is observed for phenylacetic and methylsulfonic acid derivatives, and a 13-fold improvement is seen in the case of oxamic acid derivatives (cf. **10** and **15**). Although rationalizing these small differences in potency change is difficult, modeling experiments performed on compound **10** suggest that the orientation of the N-terminal group may vary significantly between analogues containing phosphotyrosine and those which carry a phosphate group replacement (see above section on modeling and Figure 6). This could have an impact on the overall binding affinity of the ligands.

The significant increases in potency imparted by the N-terminal naphthyl group help compensate for the decrease in potency obtained by the necessary introduction of a monocharged phosphate replacement. The fact that a variety of functional groups were tolerated at the N-terminus end of our molecules could eventually have

Table 4



entry	X	K_D (μM)
16		0.04
17		5
18		2
19		4
15		3

utility since it should allow modification of the physicochemical properties of the ligands with minimal effect on binding affinities. These effects could be exploited in the development of compounds with cellular activity.

Conclusion

Using the phosphorylated dipeptide derivative **2** as a starting point, we have designed potent ligands in which the phosphate group has been replaced by monocharged, nonhydrolyzable mimics, which still bind to the protein with K_D 's in the low micromolar range. The overall expected charge (at physiological pH) of these peptidomimetic antagonists has been reduced from -3 to -2 . The drop in potency resulting from the necessity for a monocharged pY replacement was compensated for by the discovery of beneficial N-terminal modifications. These achievements represent significant steps toward the discovery of compounds with cellular activity and the development of novel therapeutics for conditions associated with anomalous intracellular signaling.

Experimental Section

Synthesis of Inhibitors. Inhibitors were prepared using standard peptide coupling procedures. In most cases, benzotriazol-1-yl-1,1,3,3-tetramethyluronium tetrafluoroborate (TBTU)²⁶ was used as coupling agent. In the case of racemization prone couplings (e.g., coupling of *N*-acylamino acid fragments), *N,N*-dicyclohexylcarbodiimide (DCC) was used, in combination with *N*-hydroxybenzotriazole (HOBT) as additive.²⁷ As depicted in Schemes 1–10 (see Supporting Information), the strategy typically involved the synthesis of protected phenylalanine derivatives incorporating protected forms of the desired phosphate group replacements. These fragments were then elaborated to full-size inhibitors and deprotected using standard protocols. In some instances, the phosphate mimic was actually constructed onto an appropriately protected full-length peptide (Schemes 6 and 7 in Supporting Information, compounds **9–11**, **13–15**).

Compound **5**, containing a previously unreported (2-carboxyethyl)-*L*-phenylalanine residue, was prepared from *N*-Boc-4-(2-propenyl)-*L*-phenylalanine benzyl ester²⁸ (**28**; Scheme 3 in Supporting Information) via hydroboration of the double bond and subsequent oxidation of the primary hydroxyl group to a carboxyl function using Jones' reagent. Derivatives containing the novel oxamic functionality as phosphate replacement were prepared from *N*-Boc-4-nitro-*L*-phenylalanine (**45**; Scheme 8 in Supporting Information) via initial protection of the carboxyl function as a benzyl ester, followed by reduction of the nitro group with iron metal in ethanolic hydrochloric acid. The oxalic moiety was then introduced by acylation of the aniline function using monomethyl oxalyl chloride. Hydrogenolysis of the benzyl ester then liberated the phenylalanine fragment suitably protected for incorporation into inhibitors.

Inhibitors were usually purified to $>95\%$ homogeneity (as determined by reversed-phase HPLC analysis in two solvent systems). All compounds were characterized by MS and ¹H NMR, and complete listings of spectral data are available in the Supporting Information.

Biological Assay. p56^{lck} SH2 protein was obtained and purified as previously reported.^{10a} K_D 's for binding are an average of duplicate experiments on two separate samples (four measurements) and were determined using a surface plasmon resonance protocol.^{10a}

Protein–Ligand Modeling. The coordinates from the crystal structure of p56^{lck} SH2 in complex with the phosphotyrosine peptide Ac-pY-E-E-I, at 1 Å resolution, were used as the starting point for calculations and docking.⁹ Protons were added where necessary, charges fixed, and calculations performed using InsightII, Discover, and the CFF95 force field (Molecular Simulations Inc., 9685 Scranton Rd, San Diego, CA 92121-3752). The fragment used for docking was prepared by taking the pY fragment directly from the above crystal structure followed by replacement of the phosphate by oxamic acid and the pY+1 side by a simple NMe amide group. Charges were determined for the fragment using the MNDO method²⁹ of obtaining ESP charges.³⁰

The fragment was docked, flexibly, into the pocket, using Autodock 2.2³¹ allowing only the non-amide portions of the oxamic acid portion freely rotatable; 50 runs of 100 cycles each were performed with an initial RT of 1000, final RT of 366, translation step of 0.2, and quaterion and torsional steps of 5. Three of these 50 runs were of low energy with the oxamic acid functionality docked deep into the phosphotyrosine binding pocket. The lowest energy position was utilized as a starting point for minimization.

Crystallographic waters were added back to the structure, and additional waters were added to solvate a 20 Å shell around the ligand. An area >15 Å away from the ligand was held fixed, while a buffer region between 15 and 12.5 Å away from the ligand was tethered to original atom positions to provide a buffer between completely free and fixed regions. A series of tethered minimizations were undertaken, successively removing more and more of the restraints in order to slowly relax the system. Eventually, the inner and buffer areas were allowed to relax completely with the outer, previously frozen region, being tethered until a gradient of 0.005 kcal/mol/Å was achieved.

The C-terminal NMe amide group was then replaced with the fragment of interest (Glu-*p*-methoxybenzyl), removing water that conflicted, followed by resolution and minimization as before to give the final, minimized model for the bound oxamic acid fragment with our modified C-terminus attached.

Small-Molecule Modeling. Phenyl oxamic acid was modeled using the PM3 semiempirical Hamiltonian^{23a} as implemented in Spartan 4.1 or 5.0 (Wavefunction Inc., 18401 Von Karman Ave, Suite 370, Irvine, CA 92612). The two non-amide torsional angles were systematically rotated, and PM3-restrained conformers were obtained. PM3-SM3 solvation energies^{23b} were then calculated for each of these conformers in an attempt to locate minima. The final minimized structure was obtained by performing a full PM3-SM3 gradient minimization on the lowest energy point calculation. A restrained

PM3-SM3 gradient minimization was also performed for the angles observed in our bound model of **10** to determine the difference in energy (1.13 kcal/mol) between the free (−207.63 kcal/mol) and bound (−206.50 kcal/mol) conformers in water.

Acknowledgment. We are grateful to Colette Bouchard and Serge Valois for analytical support.

Supporting Information Available: Detailed synthetic schemes, experimental procedures, and characterization for all compounds. This material is available free of charge via the Internet at <http://pubs.acs.org>.

References

- Brown, M. T.; Cooper, J. A. Regulation, substrates and functions of *src*. *Biochim. Biophys. Acta* **1996**, *1287*, 121–149.
- (a) Weiss, A.; Littman, D. R. Signal transduction by lymphocyte antigen receptors. *Cell* **1994**, *76*, 263–274. (b) Penninger, J. M.; Wallace, V. A.; Kishihara, K.; Mak, T. W. The role of p56^{lck} and p59^{lyn} tyrosine kinases and CD45 protein tyrosine phosphatase in T-cell development and clonal selection. *Immunol. Rev.* **1993**, *135*, 183–214.
- (a) Cohen, G. B.; Ren, R.; Baltimore, D. Modular binding domains in signal transduction proteins. *Cell* **1995**, *80*, 237–248. (b) Pawson, T. Protein modules and signaling networks. *Nature* **1995**, *373*, 573–580. (c) Lee-Fruman, K. K.; Collins, T. L.; Burakoff, S. J. Role of the *lck src* homology 2 and 3 domains in protein tyrosine phosphorylation. *J. Biol. Chem.* **1996**, *271*, 25003–25010.
- (a) Sadowski, I.; Stone, J. C.; Pawson, T. A noncatalytic domain conserved among cytoplasmic protein-tyrosine kinases modifies the kinase function and transforming activity of Fujinami sarcoma virus p130^{gag-tyr}. *Mol. Cell. Biol.* **1986**, *6*, 4396–4408. (b) Pawson, T.; Schlessinger, J. SH2 and SH3 domains. *Curr. Biol.* **1993**, *3*, 434–442 and references therein.
- Songyand, Z.; Shoelson, S. E.; Chaudhuri, M.; Gish, G.; Pawson, T.; Haser, W. G.; King, E.; Roberts, T.; Ratnofsky, S.; Lechleider, R. J.; Neel, B. G.; Birge, R. B.; Fajardo, J. E.; Chou, M. M.; Hanafusa, H.; Schaffhausen, B.; Cantley, L. C. SH2 domains recognize specific phosphopeptide sequences. *Cell* **1993**, *72*, 767–778.
- Payne, G.; Shoelson, S. E.; Gish, G. D.; Pawson, T.; Walsh, C. T. Kinetics of p56^{lck} and p60^{src} *src* homology 2 domain binding to tyrosine-phosphorylated peptides determined by a competition assay or surface plasmon resonance. *Proc. Natl. Acad. Sci. U.S.A.* **1993**, *90*, 4902–4906.
- Eck, M. J.; Shoelson, S. E.; Harrison, S. C. Recognition of a high-affinity phosphotyrosyl peptide by the *src* homology-2 domain of p56^{lck}. *Nature* **1993**, *362*, 87–91.
- (a) Eck, M. J.; Atwell, S. K.; Shoelson, S. E.; Harrison, S. C. Crystal structure of the regulatory domains of the *src*-family tyrosine kinase p56^{lck}. *Nature* **1994**, *368*, 764–769. (b) Waksman, G.; Shoelson, S. E.; Pant, N.; Cowburn, D.; Kuriyan, J. Binding of a high affinity phosphotyrosyl peptide to the *src* SH2 domain: crystal structures of the complexed and peptide-free forms. *Cell* **1993**, *72*, 779–790. (c) Lee, C. H.; Kominos, D.; Jacques, S.; Margolis, B.; Schlessinger, J.; Shoelson, S. E.; Kuriyan, J. Crystal structures of peptide complexes of the amino-terminal SH2 domain of the *src* tyrosine phosphatase. *Structure* **1994**, *2*, 423–438. (d) Gilmer, T.; Rodriguez, M.; Jordan, S.; Crosby, R.; Alligood, K.; Green, M.; Kimery, M.; Wagner, C.; Kinder, D.; Charifson, P.; Hassell, A. M.; Willard, D.; Luther, M.; Rusnak, D.; Sternbach, D. D.; Mehrotra, M.; Peel, M.; Shampine, L.; Davis, R.; Robbins, J.; Patel, I. R.; Kassel, D.; Burkhardt, W.; Moyer, M.; Bradshaw, T.; Berman, J. Peptide inhibitors of *src* SH3–SH2-phosphoprotein interactions. *J. Biol. Chem.* **1994**, *269*, 31711–31719. (e) Mikol, V.; Baumann, G.; Keller, T. H.; Manning, V.; Zurini, M. G. M. The crystal structures of the SH2 domain of p56^{lck} complexed with two phosphonopeptides suggest a gated peptide binding site. *J. Biol. Chem.* **1995**, *270*, 344–355. (f) Pascal, S. M.; Singer, A. U.; Gish, G.; Yamazaki, T.; Shoelson, S. E.; Pawson, T.; Kay, L. E.; Forman-Kay, J. D. Nuclear magnetic resonance structure of an SH2 domain of phospholipase C- γ 1 complexed with a high affinity binding peptide. *Cell* **1994**, *77*, 461–472. (g) Xu, R. X.; Word, J. M.; Davis, D. G.; Rink, M. J.; Willard, D. H., Jr.; Gampe, R. T., Jr. Solution structure of the human pp60^{src} SH2 domain complexed with a phosphorylated tyrosine pentapeptide. *Biochemistry* **1995**, *34*, 2107–2121. (h) Gay, B.; Furet, P.; Garcia-Echeverria, C.; Rahuel, J.; Chêne, P.; Fretz, H.; Schoepfer, J.; Caravatti, G. Dual specificity of *src* homology 2 domains for phosphotyrosine peptide ligands. *Biochemistry* **1997**, *36*, 5712–5718. (i) Mulhern, T. D.; Shaw, G. L.; Morton, C. J.; Day, A. J.; Campbell, I. D. The SH2 domain from the tyrosine kinase Fyn in complex with a phosphotyrosyl peptide reveals insights into domain stability and binding specificity. *Structure* **1997**, *5*, 1313–1323.
- Tong, L.; Warren, T. C.; King, J.; Betagari, R.; Rose, J.; Jakes, S. Crystal structures of the human p56^{lck} SH2 domain in complex with two short phosphotyrosyl peptides at 1.0 and 1.8 Å resolution. *J. Mol. Biol.* **1996**, *256*, 601–610 (Brookhaven Protein Data Bank accession code 1LKK).
- (a) Morelock, M. M.; Ingraham, R. H.; Betagari, R.; Jakes, S. Determination of receptor–ligand kinetic and equilibrium binding constants using surface plasmon resonance: application to the *lck* SH2 domain and phosphotyrosyl peptides. *J. Med. Chem.* **1995**, *38*, 1309–1318. (b) Cousins-Wasti, R. C.; Ingraham, R. H.; Morelock, M. M.; Grygon, C. A. Determination of affinities for *lck* SH2 binding peptides using a sensitive fluorescence assay: comparison between the pYEEIP and pYQPQP consensus sequences reveals context-dependent binding specificity. *Biochemistry* **1996**, *35*, 16746–16752.
- (a) Secrist, J. P.; Burns, L. A.; Karnitz, L.; Koretzky, G. A.; Abraham, R. T. Stimulatory effects of the protein tyrosine phosphatase inhibitor, pervanadate, on T-cell activation events. *J. Biol. Chem.* **1993**, *268*, 5886–5893. (b) O'Shea, J. J.; McVicar, D. W.; Bailey, T. L.; Burns, C.; Smyth, M. J. Activation of human peripheral blood T lymphocytes by pharmacological induction of protein-tyrosine phosphorylation. *Proc. Natl. Acad. Sci. U.S.A.* **1992**, *89*, 10306–10310. (c) Garcia-Morales, P.; Minami, Y.; Luong, E.; Klausner, R. D. Tyrosine phosphorylation in T cells is regulated by phosphatase activity: studies with phenylarsine oxide. *Proc. Natl. Acad. Sci. U.S.A.* **1990**, *87*, 9255–9259.
- (a) Beattie, J. SH2 domain protein interaction and possibilities for pharmacological intervention. *Cell. Signal.* **1996**, *8*, 75–86. (b) Botfield, M. C.; Green, J. SH2 and SH3 domains: Choreographers of multiple signaling pathways. *Annu. Rev. Med. Chem.* **1995**, *30*, 227–237 and references therein. (c) Carboxylic acids were used previously as isosteric replacement for sulfate in the context of cholecystokinin analogues: Tilley, J. W.; Danho, W.; Lovey, K.; Wagner, R.; Swistok, J.; Makofske, R.; Michalewsky, J.; Triscari, J.; Nelson, D.; Weatherford, S. Carboxylic acids and tetrazoles as isosteric replacements for sulfate in cholecystokinin analogues. *J. Med. Chem.* **1991**, *34*, 1125–1136.
- (a) Burke, T. R., Jr.; Smyth, M. S.; Otaka, A.; Nomizu, M.; Roller, P. P.; Wolf, G.; Case, R.; Shoelson, S. E. Nonhydrolyzable phosphotyrosyl mimetics for the preparation of phosphatase-resistant SH2 domain inhibitors. *Biochemistry* **1994**, *33*, 6490–6494. (b) Ye, B.; Akamatsu, M.; Shoelson, S. E.; Wolf, G.; Giorgetti-Peraldi, S.; Yan, X.; Roller, P. P.; Burke, T. R., Jr. L-O-(2-Malonyl)tyrosine: a new phosphotyrosyl mimetic for the preparation of *src* homology 2 domain inhibitory peptides. *J. Med. Chem.* **1995**, *38*, 4270–4275. (c) Burke, T. R., Jr.; Ye, B.; Akamatsu, M.; Ford, H., Jr.; Yan, X.; Kole, H. K.; Wolf, G.; Shoelson, S. E.; Roller, P. P. 4'-O-[2-(2-Fluoromalonyl)]-L-tyrosine: a phosphotyrosyl mimic for the preparation of signal transduction inhibitory peptides. *J. Med. Chem.* **1996**, *39*, 1021–1027. (d) Stankovic, C. J.; Surendran, N.; Lunney, E. A.; Plummer, M. S.; Para, K. S.; Shahripour, A.; Fergus, J. H.; Marks, J. S.; Herrera, R.; Hubbell, S. E.; Humblet, C.; Saltiel, A. R.; Stewart, B. H.; Sawyer, T. K. The role of 4-phosphonodifluoromethyl- and 4-phosphono-phenylalanine in the selectivity and cellular uptake of SH2 domain ligands. *Bioorg. Med. Chem. Lett.* **1997**, *7*, 1909–1914.
- (a) Rodriguez, M.; Crosby, R.; Alligood, K.; Gilmer, T.; Berman, J. Tripeptides as selective inhibitors of *src*-SH2 phosphoprotein interactions. *Letts. Pept. Sci.* **1995**, *2*, 1–6. (b) Saltiel, A. R.; Sawyer, T. K. Targeting signal transduction in the discovery of antiproliferative drugs. *Chem. Biol.* **1996**, *3*, 887–893. (c) Shahripour, A.; Para, K. S.; Plummer, M. S.; Lunney, E. A.; Holland, D. R.; Rubin, J. R.; Humblet, C.; Fergus, J. H.; Marks, J. S.; Saltiel, A. R.; Sawyer, T. K. Structure-based design of a novel, dipeptide ligands targeting the pp60^{src} SH2 domain. *Bioorg. Med. Chem. Lett.* **1997**, *7*, 1107–1112 and references therein. (d) Plummer, M. S.; Holland, D. R.; Shahripour, A.; Lunney, E. A.; Fergus, J. H.; Marks, J. S.; McConnel, P.; Mueller, W. T.; Sawyer, T. K. Design, synthesis and cocrystal structure of a nonpeptide *src* SH2 domain ligand. *J. Med. Chem.* **1997**, *40*, 3719–3725 and references therein. (e) Lunney, E. A.; Para, K. S.; Rubin, J. R.; Humblet, C.; Fergus, J. H.; Marks, J. S.; Sawyer, T. K. Structure-based design of a novel series of nonpeptide ligands that bind to the pp60^{src} SH2 domain. *J. Am. Chem. Soc.* **1997**, *119*, 12471–12476. (f) Charifson, P. S.; Shewchuk, L. M.; Rocque, W.; Hummel, C. W.; Jordan, S. R.; Mohr, C.; Pacofsky, G. J.; Peel, M. R.; Rodriguez, M.; Sternbach, D. D.; Consler, T. G. Peptide ligands of pp60^{src} SH2 domains: a thermodynamic and structural study. *Biochemistry* **1997**, *36*, 6283–6293. (g) Pacofsky, G. J.; Lackey, K.; Alligood, K. J.; Berman, J.; Charifson, P. S.; Crosby, R. M.; Dorsey, G. F., Jr.; Feldman, P. L.; Gilmer, T. M.; Hummel, C. W.; Jordan, S. R.; Mohr, C.; Shewchuk, L. M.; Sternbach, D. D.; Rodriguez, M. Potent dipeptide inhibitors of the pp60^{src} SH2 domain. *J. Med. Chem.* **1998**, *41*, 1894–1908. (h) Sawyer, T. K. *Src* homology-2 domains: structure, mechanisms, and drug discovery. *Biopolymers* **1998**, *47*, 243–261 and references therein.

- (15) Cell permeabilization procedures such as microinjection have been used with some success. See, for example: (a) Xiao, S.; Rose, D. W. Syp (SH-PTP2) is a positive mediator of growth factor-stimulated mitogenic signal transduction. *J. Biol. Chem.* **1994**, *269*, 21244–21428. (b) Wange, R. L. $F_2(\text{Pmp})_2\text{-TAM}\xi_3$, a novel competitive inhibitor of the binding of ZAP-70 to the T cell antigen receptor, blocks early T cell signaling. *J. Biol. Chem.* **1995**, *270*, 944–948. Isolated reports of cellular efficacy have appeared: (c) Revesz, L.; Blum, E.; Manning, U.; Demange, B. J.; Widmer, A.; Zuber, J.-F. Non-peptide ITAM mimics as ZAP-70 antagonists. *Bioorg. Med. Chem. Lett.* **1997**, *7*, 2875–2878. (d) Eaton, S. R.; Cody, W. L.; Doherty, A. M.; Holland, D. R.; Panek, R. L.; Lu, G. H.; Dahring, T. K.; Rose, D. R. Design of peptidomimetics that inhibit the association of phosphatidylinositol 3-kinase with platelet-derived growth factor- β receptor and possess cellular activity. *J. Med. Chem.* **1998**, *41*, 4329–4342. (e) Yao, Z.-J.; King, C. R.; Cao, T.; Kelley, J.; Milne, G. W. A.; Voigt, J. H.; Burke, T. R., Jr. Potent inhibition of Grb2 SH2 domain binding by nonphosphate-containing ligands. *J. Med. Chem.* **1999**, *42*, 25–35.
- (16) Llinás-Brunet, M.; Beaulieu, P. L.; Cameron, D.; Ferland, J.-M.; Gauthier, J.; Ghio, E.; Gillard, J.; Gorys, V.; Poirier, M.; Rancourt, J.; Wernic, D.; Betagari, R.; Cardozo, M.; Jakes, S.; Lukas, S.; Patel, U.; Proudfoot, J.; Moss, N. Phosphotyrosine containing dipeptides as high affinity ligands of p56 Lck SH2 domain. *J. Med. Chem.* **1999**, *42*, 722–729.
- (17) (a) Burley, S. K.; Petsko, G. A. Amino-aromatic interactions in proteins. *FEBS Lett.* **1986**, *203*, 139–143. (b) Waksman, G.; Kominos, D.; Robertson, S. C.; Pant, N.; Baltimore, D.; Birge, R. B.; Cowburn, D.; Hanafusa, H.; Mayer, B. J.; Overduin, M.; Resh, M. D.; Rios, C. B.; Silverman, L.; Kuriyan, J. Crystal structure of the phosphotyrosine recognition domain SH2 of *v-src* complexed with tyrosine phosphorylated-peptides. *Nature* **1992**, *358*, 646–653. (c) Hatada, M. H.; Lu, X.; Laird, E. R.; Green, J.; Morgenstern, J. P.; Lou, M.; Marr, C. S.; Phillips, T. B.; Ram, M. K.; Theriault, K.; Zoller, M. J.; Karas, J. L. Molecular basis for the interaction of the protein tyrosine kinase ZAP-70 with the T-cell receptor. *Nature* **1995**, *377*, 32–38.
- (18) Tong, L.; Warren, T. C.; Lukas, S.; Schembri-King, J.; Betagari, R.; Proudfoot, J.; Jakes, S. Carboxymethyl-phenylalanine as a replacement for phosphotyrosine in SH2 domain binding. *J. Biol. Chem.* **1998**, *273*, 20238–20242.
- (19) (a) Bacon, G. E.; Walker, C. R.; Speakman, J. C. Crystal structures of some acid salts of monobasic acids. Part 18. Potassium hydrogen bisphenylacetate, redetermined by neutron diffraction. *J. Chem. Soc., Perkin Trans. 2* **1977**, 979–983 (Cambridge Crystallographic Database reference code KHPAC12). (b) Hodgson, D. J.; Asplund, R. O. Phenylacetic acid. *Acta Crystallogr., Sect. C. (Cr. Str. Comm.)* **1991**, *47*, 1986–1987 (Cambridge Crystallographic Database reference code ZZZMLY01).
- (20) X-ray crystal structures of phenylpyruvate esters show the ketone carbonyl lying in the plane of the phenyl ring. See, for example: McGahren, W. J.; Martin, J. H.; Morton, G. O.; Hargreaves, R. T.; Leese, R. A.; Lovell, F. M.; Ellestad, G. A.; O'Brien, E.; Holker, J. S. E. Structure of avoparcin components. *J. Am. Chem. Soc.* **1980**, *102*, 1671–1684.
- (21) Idoux, J. P.; Kiefer, G. E.; Baker, G. R.; Puckett, W. E.; Spence, F. J., Jr.; Simmons, K. S.; Constant, R. B.; Watlock, D. J.; Fuhrman, S. L. Mode of electronic effect transmission via the amide bond. *J. Org. Chem.* **1980**, *45*, 441–444.
- (22) Cheney, B. V.; Christoffersen, R. E. Structure–activity correlation for a series of anti-allergy agents. 3. Development of a quantitative model. *J. Med. Chem.* **1983**, *26*, 726–737.
- (23) (a) Stewart, J. J. P. Optimization of parameters for semiempirical methods. II. Applications. *J. Comput. Chem.* **1989**, *10*, 221–264. (b) Cramer, C. J.; Truhlar, D. G. AM1-SM2 and PM3-SM3 parametrized SCF solvation models for free energies in aqueous solution. *J. Comput.-Aided Mol. Des.* **1992**, *6*, 629–666.
- (24) Unpublished results.
- (25) (a) Furet, P.; Gay, B.; Garcia-Echeverria, C.; Rahuel, J.; Fretz, H.; Schoepfer, J.; Caravatti, G. Discovery of 3-aminobenzoyloxy-carbonyl as an N-terminal group conferring high affinity to the minimal phosphopeptide sequence recognized by the Grb2-SH2 domain. *J. Med. Chem.* **1997**, *40*, 3551–3556. (b) Rahuel, J.; Garcia-Echeverria, C.; Furet, P.; Strauss, A.; Caravatti, G.; Fretz, H.; Schoepfer, J.; Gay, B. Structural basis for the high affinity of amino-aromatic SH2 phosphopeptide ligands. *J. Mol. Biol.* **1998**, *279*, 1013–1022.
- (26) Knorr, R.; Trzeciak, A.; Bannwarth, W.; Gillessen, D. New coupling reagents in peptide synthesis. *Tetrahedron Lett.* **1989**, *30*, 1927–1930.
- (27) (a) Bodanszky, M. In *Principles of Peptide Synthesis*; Springer-Verlag: New York, 1984. (b) *The Peptides*; Gross, E., Meienhofer, J., Eds.; Academic Press: New York, 1979; Vol 1.
- (28) Tilley, J. W.; Sarabu, R.; Wagner, R.; Mulkerins, K. Preparation of carboalkoxyphenylalanine derivatives from tyrosine. *J. Org. Chem.* **1990**, *55*, 906–910.
- (29) Dewar, M. J. S.; Thiel, W. Ground state of molecules. 38. The MNDO method. Approximations and parameters. *J. Am. Chem. Soc.* **1977**, *99*, 4899–4907.
- (30) Besler, B. H.; Merz, K. M., Jr.; Kollman, P. A. Atomic charges derived from semiempirical methods. *J. Comput. Chem.* **1990**, *11*, 431–439.
- (31) Goodsell, D. S.; Olson, A. J. Automated docking of substrates to proteins by simulated annealing. *Proteins: Struct. Funct. Genet.* **1990**, *8*, 195–202.

JM980676T